Supporting Information

Exploring Hyperfine Coupling in Molecular Qubits

Joan Cardona,[a] Àlex Solé,[a,b] Pablo Mella,[c] Daniel Aravena,[c] Javier Ruiz-Hidalgo,[b] Silvia Gómez-Coca[a] and Eliseo Ruiz[a]

[a] Departament de Química Inorgànica i Orgànica and Institut de Recerca de Química Teòrica i Computacional, Universitat de Barcelona, Diagonal 645, 08028 Barcelona, Spain.
[b] Department of Image Processing Group - Signal Theory and Communications Department, Universitat Politècnica de Catalunya, Jordi Girona 1-3, 08034 Barcelona, Spain.
[c] Departamento de Química de los Materiales, Facultad de Química y Biología, Universidad de Santiago de Chile, Casilla 40, Correo 33, Santiago, Chile.

Table of Contents

S1. Solvation Effects

EPR measurements can be performed using either a diamagnetic matrix or a frozen solution. When using a diamagnetic matrix, the central transition metal in the compound of interest is substituted with a diamagnetic element to create an isostructural complex. This approach eliminates contributions from the metal centre to the EPR spectrum. However, measurements in frozen solution are also possible. In such cases, careful consideration of external stimuli is crucial for reproducing experimental values. For instance. [CpTi(cot)] and $[V(C_8S_8)_3]^{2-}$ were measured in frozen solutions of toluene and CS_2, respectively. To achieve such effects, first an optimization of both structures was done using Gaussian 16, employing BP86/def2-TZVP and the Polarized Continuum Model (PCM). Then, HFC constants were calculated as indicated in the Computational Details section employing the Conductor-like Screening Model (COSMO). In conclusion, no significant changes were observed in the EPR spectra of the modified compounds. According to other compound references, diamagnetic matrices were prepared for compounds $[V(dmit)_3]^{2-}$, $[Cu(mnt)_2]^{2-}$ and $[VO(dmit)_2]^{2-}$ to conduct EPR measurements.

Table S1. HFC constants comparison between solvent-free, solvation model and experimental values.

Compound	Method	$A_\perp$ (MHz)	$A_\perp$ (MHz)	$A_\parallel$ (MHz)
$[V(C_8S_8)_3]^{2-}$	Solvent-free[a]	-294.7	-134.7	-5.7
	Solvation Model	-265.1	-158.1	25.7
	Experimental	**-258.0**	**-258.0**	**6.0**
[CpTi(cot)]	Solvent-free[a]	42.4	42.5	-5.8
	Solvation Model	40.8	40.8	-6.9
	Experimental	**52.4**	**52.4**	**ca. 5**

[a] Solvent-free approach calculation was performed using uncontracted ANO-DK3 basis set alongside B3LYP functional.

S2. Hyperfine Benchmark Assessment

Table S2. Computed hyperfine coupling constant values split into both perpendicular (⊥) and parallel (∥) components and the mean absolute percentage logarithmic error of $[Cu(mnt)_2]^{2-}$. Experimental values reported in the literature were given as absolute magnitudes.

Functional	Basis	$A_\perp$ (MHz)	$A_\perp$ (MHz)	$A_\parallel$ (MHz)	MAPLE (%)
B3LYP	ANO-DK3/IGLO-III	-20.3	-28.7	-305.5	24.8
	x2c-TZVPPall/IGLO-III	168.7	163.0	-251.7	8.4
	x2c-TZVPPall	165.9	160.2	-253.2	8.2
	x2c-TZVPall	162.1	156.6	-249.9	7.9
	x2c-QZVPPall	-103.3	-97.9	-504.0	2.3
	x2c-QZVPPall-s	-103.5	-98.0	-500.4	2.2
	def2-QZVPP	-42.6	-48.0	-464.7	13.8
	UGBS unc.	-80.3	-85.9	-495.8	5.0
	ANO-DK3 unc.	-85.7	-91.5	-497.9	4.0
	ANO-DK3 *s* unc.	-177.7	-189.8	-453.8	6.7
	ZORA – ANO-DK3 unc.	-80.1	-85.3	-520.4	5.2
	Non-relativistic – Def2-QZVPP	-87.2	-92.3	-537.7	4.2
ωB97X	ANO-DK3/IGLO-III	-63.9	-69.6	-390.6	9.3
	x2c-TZVPPall/IGLO-III	96.5	92.5	-367.1	4.8
	x2c-TZVPPall	93.6	89.6	-368.5	5.2
	x2c-QZVPPall	-183.0	-178.7	-627.7	7.2
	def2-QZVPP	-104.9	-108.8	-572.1	2.1
	ANO-DK3 Unc.	-161.0	-165.5	-611.7	5.6
PBE40	ANO-DK3/IGLO-III	-53.1	-59.3	-377.9	11.9
	x2c-TZVPPall/IGLO-III	212.4	207.7	-287.4	11.0
	x2c-TZVPPall	208.7	204.0	-289.7	10.7
	x2c-QZVPPall	-138.8	-143.6	-617.5	3.6
	def2-QZVPP	-61.3	-65.9	-564.5	9.3
	ANO-DK3 Unc.	-124.4	-129.1	-597.9	2.0
PBE0	ANO-DK3/IGLO-III	-34.0	-41.3	-331.2	18.2
	x2c-TZVPPall/IGLO-III	158.9	154.1	-283.2	7.0
	x2c-TZVPPall	155.6	150.8	-285.1	6.7
	x2c-QZVPPall	-134.4	-129.8	-555.6	2.1
	def2-QZVPP	-64.5	-69.0	-509.0	8.1
	ANO-DK3 Unc.	-114.5	-119.1	-544.6	0.7
Experimental		**118.0**	**118.0**	**500.0**	

Table S3. Computed hyperfine coupling constant values split into both perpendicular (⊥) and parallel (∥) components and the mean absolute percentage logarithmic error of $[V(dmit)_3]^{2-}$. Experimental values reported in the literature were given as absolute magnitudes.

Functional	Basis	$A_{\perp}$ (MHz)	$A_{\perp}$ (MHz)	$A_{\parallel}$ (MHz)	MAPLE (%)
B3LYP	ANO-DK3/IGLO-III	227.4	67.9	-2.4	34.5
	x2c-TZVPPall/IGLO-III	236.9	54.0	-26.8	13.9
	x2c-TZVPPall	242.7	57.0	-24.7	14.1
	x2c-TZVPall	254.8	71.6	-8.7	21.9
	x2c-QZVPPall	-260.7	-182.2	-3.6	23.9
	x2c-QZVPPall-s	-257.4	-179.7	-2.9	26.2
	def2-QZVPP	-253.7	-169.8	20.6	8.8
	UGBS Unc.	-273.2	-200.1	-26.5	5.1
	ANO-DK3 Unc.	-275.9	-204.1	-31.9	3.3
	ANO-DK3 s Unc.	-311.1	-247.6	-93.8	8.4
	ZORA – ANO-DK3 Unc.	-273.8	-203.1	-32.4	3.2
	Non-relativistic – Def2-QZVPP	-269.7	-187.1	2.1	28.7
ωB97X	ANO-DK3/IGLO-III	262.6	79.8	5.0	26.0
	x2c-TZVPPall/IGLO-III	279.9	61.6	-27.7	11.8
	x2c-TZVPPall	287.3	66.3	-24.3	12.4
	x2c-QZVPPall	-220.2	-132.2	82.4	11.7
	def2-QZVPP	-221.4	-128.2	99.1	13.5
	ANO-DK3 Unc.	-240.5	-161.7	40.0	3.4
PBE40	ANO-DK3/IGLO-III	204.8	88.5	41.0	8.3
	x2c-TZVPPall/IGLO-III	236.9	54.0	-26.7	13.9
	x2c-TZVPPall	180.6	-72.1	6.0	27.2
	x2c-QZVPPall	-316.6	-242.3	-76.9	6.6
	def2-QZVPP	-305.5	-225.9	-48.4	2.0
	ANO-DK3 Unc.	-339.6	-279.4	-141.9	13.4
PBE0	ANO-DK3/IGLO-III	233.0	83.9	17.6	15.1
	x2c-TZVPPall/IGLO-III	187.4	-63.8	13.4	20.5
	x2c-TZVPPall	194.4	-60.9	17.4	18.2
	x2c-QZVPPall	-284.1	-209.2	-39.7	1.0
	def2-QZVPP	-273.8	-193.7	-12.5	12.1
	ANO-DK3 Unc.	-304.0	-236.1	-75.3	6.0
Experimental		**299.0**	**230.0**	**40.0**	

Table S4. Computed hyperfine coupling constant values split into both perpendicular (⊥) and parallel (∥) components and the mean absolute percentage logarithmic error of $[V(C_8S_8)_3]^{2-}$.

Functional	Basis	$A_\perp$ (MHz)	$A_\perp$ (MHz)	$A_\parallel$ (MHz)	MAPLE (%)
B3LYP	ANO-DK3/IGLO-III	216.0	93.6	-61.8	50.5
	x2c-TZVPPall/IGLO-III	225.6	94.2	-76.8	54.3
	x2c-TZVPPall	228.3	96.1	-75.7	53.8
	x2c-TZVPall	240.1	108.8	-60.3	48.5
	x2c-QZVPPall	-281.9	-116.2	10.7	16.1
	x2c-QZVPPall-s	-278.5	-114.5	11.0	16.6
	def2-QZVPP	-279.6	-102.6	33.0	37.7
	UGBS Unc.	-291.3	-132.8	-3.0	17.6
	ANO-DK3 Unc.	-294.7	-134.7	-5.7	5.5
	ANO-DK3 s Unc.	-323.8	-171.4	-48.4	42.6
	ZORA – ANO-DK3 Unc.	-292.2	-134.6	-6.8	7.0
	Non-relativistic – Def2-QZVPP	-292.8	-118.3	16.1	23.8
ωB97X	ANO-DK3/IGLO-III	247.5	107.8	-63.2	49.3
	x2c-TZVPPall/IGLO-III	260.5	109.0	-81.5	53.8
	x2c-TZVPPall	263.5	111.7	-79.6	53.3
	x2c-QZVPPall	-254.0	79.5	-67.3	52.1
	def2-QZVPP	-258.2	95.0	-60.6	49.0
	ANO-DK3 Unc.	-273.0	-96.1	51.3	46.2
PBE40	ANO-DK3/IGLO-III	227.8	106.8	-47.4	44.5
	x2c-TZVPPall/IGLO-III	190.2	-125.9	51.1	46.0
	x2c-TZVPPall	263.5	111.9	-79.8	53.3
	x2c-QZVPPall	-331.3	-158.3	-26.1	31.8
	def2-QZVPP	-327.7	-143.1	1.0	37.6
	ANO-DK3 Unc.	-347.7	-187.5	-56.3	45.4
PBE0	ANO-DK3/IGLO-III	224.0	103.0	-49.3	45.6
	x2c-TZVPPall/IGLO-III	186.1	-110.0	57.0	49.0
	x2c-TZVPPall	189.3	-108.2	59.6	49.8
	x2c-QZVPPall	-301.3	-140.1	-15.0	21.6
	def2-QZVPP	-296.4	-123.5	9.9	14.6
	ANO-DK3 Unc.	-316.8	-161.9	-36.6	37.7
Experimental		**-258.0**	**-258.0**	**6.0**	

Table S5. Computed hyperfine coupling constant values split into both perpendicular (⊥) and parallel (∥) components, and the mean absolute percentage logarithmic error of $[VO(dmit)_2]^{2-}$. Experimental values reported in the literature were given as absolute magnitudes.

Functional	Basis	$A_\perp$ (MHz)	$A_\perp$ (MHz)	$A_\parallel$ (MHz)	MAPLE (%)
B3LYP	ANO-DK3/IGLO-III	135.6	124.9	-163.3	5.4
	x2c-TZVPPall/IGLO-III	130.5	122.3	-180.4	5.3
	x2c-TZVPPall	132.5	124.6	-178.3	5.1
	x2c-TZVPall	147.0	139.1	-159.9	6.3
	x2c-QZVPPall	-77.4	-70.4	-369.5	8.6
	x2c-QZVPPall-s	-69.8	-76.5	-365.7	8.8
	def2-QZVPP	-53.4	-45.6	-363.2	14.2
	WTBS/UGBS Unc.	-81.9	-74.5	-376.3	7.8
	ANO-DK3 Unc.	-86.0	-78.2	-379.8	7.1
	ANO-DK3 s Unc.	-130.2	-118.3	-426.6	1.1
	ZORA – ANO-DK3 Unc.	-86.7	-79.0	-376.8	7.0
	Non-relativistic – Def2-QZVPP	-75.4	-68.0	-382.5	8.9
ωB97X	ANO-DK3/IGLO-III	136.5	126.8	-174.8	4.9
	x2c-TZVPPall/IGLO-III	138.2	129.9	-189.7	4.4
	x2c-TZVPPall	91.7	83.9	-214.2	9.3
	x2c-QZVPPall	-42.6	-35.1	-353.5	17.8
	def2-QZVPP	-23.1	-15.4	-349.9	27.6
	ANO-DK3 Unc.	-61.8	-54.5	-369.9	11.9
PBE40	ANO-DK3/IGLO-III	131.5	120.2	-179.2	5.4
	x2c-TZVPPall/IGLO-III	76.5	68.7	-246.3	11.1
	x2c-TZVPPall	78.7	71.2	-244.2	10.7
	x2c-QZVPPall	-131.8	-125.0	-434.8	0.8
	def2-QZVPP	-101.8	-94.1	-423.8	4.3
	ANO-DK3 Unc.	-145.6	-138.6	-446.3	1.3
PBE0	ANO-DK3/IGLO-III	138.3	126.9	-161.9	5.3
	x2c-TZVPPall/IGLO-III	89.7	81.7	-216.2	9.6
	x2c-TZVPPall	91.7	83.9	-214.2	9.3
	x2c-QZVPPall	-102.3	-95.3	-389.2	4.4
	def2-QZVPP	-75.8	-67.9	-380.8	8.9
	ANO-DK3 Unc.	-114.0	-106.5	-401.8	2.7
Experimental		**138.0**	**128.0**	**413.0**	

Table S6. Computed hyperfine coupling constant values split into both perpendicular (⊥) and parallel (∥) components, and the mean absolute percentage logarithmic error of [CpTi(cot)]. Experimental values reported in the literature were given as absolute magnitudes.

Functional	Basis	$A_{\perp}$ (MHz)	$A_{\perp}$ (MHz)	$A_{\parallel}$ (MHz)	MAPLE (%)
B3LYP	ANO-DK3/IGLO-III	-3.6	-3.5	-51.8	93.8
	x2c-TZVPPall/IGLO-III	16.0	16.1	-33.9	59.6
	x2c-TZVPPall	16.4	16.5	-32.3	58.1
	x2c-TZVPall	9.0	9.1	-40.3	72.8
	x2c-QZVPPall	39.2	39.3	-9.1	17.3
	x2c-QZVPPall-s	73.2	73.3	19.7	34.0
	def2-QZVPP	-13.1	38.0	38.1	56.4
	WTBS/UGBS Unc.	41.8	41.9	-6.4	8.9
	ANO-DK3 Unc.	42.4	42.5	-5.8	6.7
	ANO-DK3 s Unc.	47.4	47.2	-3.4	10.0
	ZORA – ANO-DK3 Unc.	42.0	42.1	-5.5	5.5
	Non-relativistic – Def2-QZVPP	40.6	40.7	-10.1	18.8
ωB97X	ANO-DK3/IGLO-III	-7.2	-7.1	-57.1	83.9
	x2c-TZVPPall/IGLO-III	9.8	9.9	-41.2	71.9
	x2c-TZVPPall	10.2	10.3	-40.5	70.9
	x2c-QZVPPall	26.9	27.1	-23.2	43.0
	def2-QZVPP	27.0	27.1	-25.6	45.0
	ANO-DK3 Unc.	31.7	31.8	-17.4	34.3
PBE40	ANO-DK3/IGLO-III	2.1	2.2	-46.8	100.0
	x2c-TZVPPall/IGLO-III	29.4	29.6	-20.7	39.1
	x2c-TZVPPall	29.9	30.1	-20.0	38.1
	x2c-QZVPPall	50.1	50.3	2.0	19.8
	def2-QZVPP	48.0	48.1	2.9	12.6
	ANO-DK3 Unc.	53.5	53.6	6.0	4.3
PBE0	ANO-DK3/IGLO-III	-2.1	-2.0	-49.4	101.8
	x2c-TZVPPall/IGLO-III	24.8	24.9	-23.4	44.5
	x2c-TZVPPall	25.4	25.4	-22.7	43.5
	x2c-QZVPPall	44.4	44.5	-2.1	21.1
	def2-QZVPP	42.7	42.8	-6.8	9.6
	ANO-DK3 Unc.	47.7	47.8	1.6	24.8
Experimental		**52.4**	**52.4**	**ca. 5**	

Table S7. Mean absolute percentile logarithmic error (MAPLE) for the methodologies shown in Figure 2.

Relativistic Treatment	Functional	Basis	MAPLE
x2c	B3LYP	ANO-DK3/IGLO-III	41.8
x2c	B3LYP	x2c –TZVPPall	27.9
x2c	B3LYP	x2c – QZVPPall	13.6
x2c	B3LYP	def2 – QZVPP	26.2
x2c	B3LYP	ANO – DK3 unc.	5.3
x2c	ωB97X	ANO-DK3|IGLO-III	34.7
x2c	ωB97X	x2c-TZVPPall|IGLO-III	29.3
x2c	ωB97X	x2c-TZVPPall	30.2
x2c	ωB97X	x2c-QZVPPall	26.4
x2c	ωB97X	def2-QZVPP	27.4
x2c	ωB97X	ANO-DK3 Unc.	20.3
x2c	PBE40	ANO-DK3|IGLO-III	34.0
x2c	PBE40	x2c-TZVPPall|IGLO-III	24.2
x2c	PBE40	x2c-TZVPPall	28.0
x2c	PBE40	x2c-QZVPPall	12.5
x2c	PBE40	def2-QZVPP	13.2
x2c	PBE40	ANO-DK3 Unc.	13.3
x2c	PBE0	ANO-DK3|IGLO-III	37.2
x2c	PBE0	x2c-TZVPPall|IGLO-III	26.1
x2c	PBE0	x2c-TZVPPall	25.5
x2c	PBE0	x2c-QZVPPall	10.0
x2c	PBE0	def2-QZVPP	10.7
x2c	PBE0	ANO-DK3 Unc.	14.4
ZORA	B3LYP	ANO-DK3U	5.5
Non-Rel.	B3LYP	Def2-QZVPP	16.9

S3. g-factor Benchmark Assessment

Table S8. Computed $[Cu(mnt)_2]^{2-}$ g-values and mean absolute error.

Functional	Basis	g_x	g_y	g_z	MAE
B3LYP	ANO-DK3/IGLO-III	2.0106	2.0207	2.0428	0.0213
	x2c-TZVPPall/IGLO-III	2.0202	2.0196	2.0717	0.0088
	x2c-TZVPPall	2.0201	2.0198	2.0719	0.0087
	x2c-TZVPall	2.0200	2.0198	2.0714	0.0089
	x2c-QZVPPall	2.0202	2.0198	2.0729	0.0083
	x2c-QZVPPall-s	2.0202	2.0198	2.0729	0.0083
	def2-QZVPP	2.0198	2.0203	2.0725	0.0084
	UGBS Unc.	2.0265	2.0254	2.0865	0.0042
	ANO-DK3 Unc.	2.0247	2.0236	2.0829	0.0042
	ANO-DK3 s Unc.	2.0126	2.0339	2.0557	0.0194
	ZORA – ANO-DK3 Unc.	2.0256	2.0273	2.0843	0.0052
ωB97X	ANO-DK3/IGLO-III	2.0133	2.0170	2.0532	0.0181
	x2c-TZVPPall/IGLO-III	2.0248	2.0233	2.0884	0.0023
	x2c-TZVPPall	2.0246	2.0229	2.0885	0.0020
	x2c-QZVPPall	2.0245	2.0232	2.0896	0.0017
	def2-QZVPP	2.0231	2.0248	2.0892	0.0019
	ANO-DK3 Unc.	2.0283	2.0304	2.1009	0.0072
PBE40	ANO-DK3/IGLO-III	2.0142	2.0175	2.0586	0.0159
	x2c-TZVPPall/IGLO-III	2.0339	2.0310	2.1220	0.0163
	x2c-TZVPPall	2.0337	2.0307	2.1219	0.0161
	x2c-QZVPPall	2.0340	2.0308	2.1229	0.0166
	def2-QZVPP	2.0310	2.0343	2.1240	0.0171
	ANO-DK3 Unc.	2.0365	2.0395	2.1356	0.0246
PBE0	ANO-DK3/IGLO-III	2.0117	2.0188	2.0464	0.0203
	x2c-TZVPPall/IGLO-III	2.0234	2.0215	2.0822	0.0041
	x2c-TZVPPall	2.0233	2.0216	2.0822	0.0040
	x2c-QZVPPall	2.0215	2.0233	2.0835	0.0036
	def2-QZVPP	2.0215	2.0237	2.0834	0.0038
	ANO-DK3 Unc.	2.0261	2.0285	2.0946	0.0038
Experimental		**2.0227**	**2.0227**	**2.0925**	

Table S9. Computed $[V(dmit)_3]^{2-}$ g-values and mean absolute error.

Functional	Basis	g_x	g_y	g_z	MAE
B3LYP	ANO-DK3/IGLO-III	1.9587	1.9628	1.9643	0.0104
	x2c-TZVPPall/IGLO-III	1.9610	1.9653	1.9672	0.0078
	x2c-TZVPPall	1.9606	1.9647	1.9672	0.0082
	x2c-TZVPall	1.9603	1.9644	1.9669	0.0085
	x2c-QZVPPall	1.9606	1.9671	1.9645	0.0083
	x2c-QZVPPall-s	1.9607	1.9647	1.9672	0.0081
	def2-QZVPP	1.9600	1.9641	1.9666	0.0088
	UGBS Unc.	1.9632	1.9529	1.9567	0.0162
	ANO-DK3 Unc.	1.9635	1.9528	1.9564	0.0164
	ANO-DK3 s Unc.	1.9396	1.9414	1.9529	0.0277
	ZORA – ANO-DK3 Unc.	1.9542	1.9581	1.9655	0.0131
ωB97X	ANO-DK3/IGLO-III	1.9449	1.9512	1.9569	0.0213
	x2c-TZVPPall/IGLO-III	1.9522	1.9584	1.9632	0.0144
	x2c-TZVPPall	1.9515	1.9579	1.9636	0.0147
	x2c-QZVPPall	1.9512	1.9578	1.9632	0.0149
	def2-QZVPP	1.9499	1.9569	1.9628	0.0158
	ANO-DK3 Unc.	1.9423	1.9503	1.9575	0.0223
PBE40	ANO-DK3/IGLO-III	1.8595	1.9252	1.9494	0.0610
	x2c-TZVPPall/IGLO-III	1.9611	1.9653	1.9673	0.0078
	x2c-TZVPPall	1.9152	1.9363	1.9454	0.0400
	x2c-QZVPPall	1.9144	1.9369	1.9465	0.0397
	def2-QZVPP	1.9124	1.9348	1.9447	0.0417
	ANO-DK3 Unc.	1.8897	1.9216	1.9397	0.0553
PBE0	ANO-DK3/IGLO-III	1.9481	1.9563	1.9594	0.0177
	x2c-TZVPPall/IGLO-III	1.9559	1.9603	1.9608	0.0133
	x2c-TZVPPall	1.9555	1.9601	1.9603	0.0137
	x2c-QZVPPall	1.9543	1.9589	1.9596	0.0147
	def2-QZVPP	1.9547	1.9593	1.9598	0.0144
	ANO-DK3 Unc.	1.9470	1.9554	1.9514	0.0211
Experimental		**1.9610**	**1.9710**	**1.9850**	

Table S10. Computed $[V(C_8S_8)_3]^{2-}$ g-values and mean absolute error.

Fuctional	Basis	g_x	g_y	g_z	MAE
B3LYP	ANO-DK3/IGLO-III	1.9783	1.9724	1.9669	0.013
	x2c-TZVPPall/IGLO-III	1.9810	1.9714	1.9672	0.012
	x2c-TZVPPall	1.9811	1.9713	1.9668	0.012
	x2c-TZVPall	1.9808	1.9710	1.9665	0.013
	x2c-QZVPPall	1.9811	1.9715	1.9668	0.012
	x2c-QZVPPall-s	1.9811	1.9714	1.9667	0.012
	def2-QZVPP	1.9808	1.9709	1.9661	0.013
	UGBS Unc.	1.9776	1.9660	1.9587	0.018
	ANO-DK3 Unc.	1.9785	1.9658	1.9596	0.017
	ANO-DK3 s Unc.	1.9718	1.9558	1.9483	0.027
	ZORA – ANO-DK3 Unc.	1.9602	1.9660	1.9798	0.022
ωB97X	ANO-DK3/IGLO-III	1.9748	1.9677	1.9560	0.019
	x2c-TZVPPall/IGLO-III	1.9803	1.9668	1.9580	0.017
	x2c-TZVPPall	1.9804	1.9667	1.9571	0.017
	x2c-QZVPPall	1.9803	1.9667	1.9571	0.017
	def2-QZVPP	1.9800	1.9658	1.9561	0.018
	ANO-DK3 Unc.	1.9773	1.9599	1.9476	0.024
PBE40	ANO-DK3/IGLO-III	1.9580	1.9497	1.9413	0.036
	x2c-TZVPPall/IGLO-III	1.9660	1.9593	1.9478	0.028
	x2c-TZVPPall	1.9804	1.9666	1.9576	0.017
	x2c-QZVPPall	1.9663	1.9594	1.9509	0.026
	def2-QZVPP	1.9653	1.9572	1.9460	0.029
	ANO-DK3 Unc.	1.9588	1.9508	1.9359	0.037
PBE0	ANO-DK3/IGLO-III	1.9724	1.9691	1.9615	0.018
	x2c-TZVPPall/IGLO-III	1.9772	1.9690	1.9636	0.015
	x2c-TZVPPall	1.9773	1.9691	1.9633	0.015
	x2c-QZVPPall	1.9769	1.9678	1.9613	0.017
	def2-QZVPP	1.9768	1.9685	1.9624	0.016
	ANO-DK3 Unc.	1.9744	1.9628	1.9550	0.021
Experimental		**1.9920**	**1.9920**	**1.9720**	

Table S11. Computed $[VO(dmit)_2]^{2-}$ g-values and mean absolute error.

Fuctional	Basis	g_x	g_y	g_z	MAE
B3LYP	ANO-DK3/IGLO-III	1.9855	1.9881	1.9787	0.0031
	x2c-TZVPPall/IGLO-III	1.9857	1.9879	1.9762	0.0022
	x2c-TZVPPall	1.9856	1.9880	1.9761	0.0022
	x2c-TZVPall	1.9855	1.9878	1.9759	0.0022
	x2c-QZVPPall	1.9855	1.9878	1.9762	0.0023
	x2c-QZVPPall-s	1.9855	1.9879	1.9763	0.0023
	def2-QZVPP	1.9877	1.9853	1.9759	0.0034
	WTBS/UGBS Unc.	1.9873	1.9838	1.9722	0.0026
	ANO-DK3 Unc.	1.9875	1.9838	1.9719	0.0015
	ANO-DK3 s Unc.	1.9830	1.9884	1.9653	0.0027
	ZORA – ANO-DK3 Unc.	1.9890	1.9857	1.9734	0.0020
ωB97X	ANO-DK3/IGLO-III	1.9844	1.9865	1.9742	0.0024
	x2c-TZVPPall/IGLO-III	1.9846	1.9864	1.9716	0.0015
	x2c-TZVPPall	1.9845	1.9869	1.9744	0.0023
	x2c-QZVPPall	1.9844	1.9863	1.9716	0.0016
	def2-QZVPP	1.9861	1.9842	1.9712	0.0017
	ANO-DK3 Unc.	1.9857	1.9829	1.9671	0.0028
PBE40	ANO-DK3/IGLO-III	1.9801	1.9826	1.9719	0.0044
	x2c-TZVPPall/IGLO-III	1.9832	1.9811	1.9686	0.0037
	x2c-TZVPPall	1.9811	1.9833	1.9686	0.0037
	x2c-QZVPPall	1.9811	1.9833	1.9692	0.0035
	def2-QZVPP	1.9804	1.9826	1.9684	0.0042
	ANO-DK3 Unc.	1.9784	1.9818	1.9641	0.0066
PBE0	ANO-DK3/IGLO-III	1.9842	1.9869	1.9768	0.0032
	x2c-TZVPPall/IGLO-III	1.9845	1.9868	1.9745	0.0024
	x2c-TZVPPall	1.9845	1.9869	1.9744	0.0023
	x2c-QZVPPall	1.9844	1.9868	1.9746	0.0025
	def2-QZVPP	1.9841	1.9865	1.9742	0.0025
	ANO-DK3 Unc.	1.9826	1.9862	1.9701	0.0018
Experimental		**1.9860**	**1.9880**	**1.9700**	

Table S12. Computed [CpTi(cot)] g-values and mean absolute error.

Fuctional	Basis	g_x	g_y	g_z	MAE
B3LYP	ANO-DK3/IGLO-III	1.9765	1.9771	2.0004	0.0034
	x2c-TZVPPall/IGLO-III	1.9770	1.9773	2.0004	0.0036
	x2c-TZVPPall	1.9770	1.9775	2.0004	0.0037
	x2c-TZVPall	1.9768	1.9773	2.0004	0.0036
	x2c-QZVPPall	1.9768	1.9772	2.0003	0.0036
	x2c-QZVPPall-s	1.9647	1.9652	2.0005	0.0049
	def2-QZVPP	1.9764	1.9769	2.0003	0.0033
	WTBS/UGBS Unc.	1.9749	1.9754	2.0002	0.0024
	ANO-DK3 Unc.	1.9750	1.9756	2.0001	0.0025
	ANO-DK3 s Unc.	1.9658	1.9665	1.9997	0.0043
	ZORA – ANO-DK3 Unc.	1.9769	1.9773	2.0016	0.0036
ωB97X	ANO-DK3/IGLO-III	1.9746	1.9749	2.0003	0.0021
	x2c-TZVPPall/IGLO-III	1.9756	1.9759	2.0004	0.0027
	x2c-TZVPPall	1.9752	1.9758	2.0004	0.0025
	x2c-QZVPPall	1.9748	1.9752	2.0004	0.0022
	def2-QZVPP	1.9743	1.9747	2.0004	0.0019
	ANO-DK3 Unc.	1.9732	1.9737	2.0001	0.0013
PBE40	ANO-DK3/IGLO-III	1.9728	1.9733	2.0003	0.0009
	x2c-TZVPPall/IGLO-III	1.9745	1.9746	2.0005	0.0019
	x2c-TZVPPall	1.9744	1.9746	2.0004	0.0019
	x2c-QZVPPall	1.9751	1.9750	2.0003	0.0023
	def2-QZVPP	1.9735	1.9742	2.0004	0.0014
	ANO-DK3 Unc.	1.9713	1.9726	2.0000	0.0008
PBE0	ANO-DK3/IGLO-III	1.9768	1.9772	2.0004	0.0035
	x2c-TZVPPall/IGLO-III	1.9769	1.9779	2.0005	0.0038
	x2c-TZVPPall	1.9768	1.9776	2.0004	0.0037
	x2c-QZVPPall	1.9772	1.9780	2.0003	0.0040
	def2-QZVPP	1.9764	1.9769	2.0004	0.0033
	ANO-DK3 Unc.	1.9760	1.9762	2.0001	0.0030
Experimental		**1.9720**	**1.9720**	**2.0010**	

Table S13. Computed g-values and mean absolute error for compounds **6 – 12**.

Compound	Method	g_x	g_y	g_z	MAE
[Cu(Pc)]	x2c – B3LYP / x2c-QZVPPall	2.0378	2.0378	2.1254	0.0324
	x2c – B3LYP / ANO-DK3 Unc.	2.0416	2.0416	2.1333	0.0272
	ZORA – B3LYP / ANO-DK3 Unc.	2.0439	2.0440	2.1342	0.0254
	Experimental	**2.0496**	**2.0496**	**2.1990**	
$[V(C_6Br_4O_2)_3]^{2-}$	x2c – B3LYP / x2c-QZVPPall	1.9514	1.9491	1.9912	0.0142
	x2c – B3LYP / ANO-DK3 Unc.	1.9479	1.9451	1.9905	0.0115
	ZORA – B3LYP / ANO-DK3 Unc.	1.9465	1.9485	1.9925	0.0128
	Experimental	**1.9380**	**1.9210**	**1.9900**	
$[V(C_6H_4O_2)_3]^{2-}$	x2c – B3LYP / x2c-QZVPPall	1.9534	1.9491	1.9913	0.0109
	x2c – B3LYP / ANO-DK3 Unc.	1.9469	1.9421	1.9905	0.0065
	ZORA – B3LYP / ANO-DK3 Unc.	1.9505	1.9459	1.9936	0.0097
	Experimental	**1.9420**	**1.9280**	**1.9910**	
[Cu(acacen)]	x2c – B3LYP / x2c-QZVPPall	2.0345	2.0375	2.1346	0.0211
	x2c – B3LYP / ANO-DK3 Unc.	2.0384	2.0405	2.1426	0.0162
	ZORA – B3LYP / ANO-DK3 Unc.	2.0414	2.0434	2.1435	0.0139
	Experimental	**2.0450**	**2.0450**	**2.1800**	
[Cu(tmtaa)]	x2c – B3LYP / x2c-QZVPPall	2.0327	2.0285	2.1335	0.0192
	x2c – B3LYP / ANO-DK3 Unc.	2.0353	2.0327	2.1392	0.0196
	ZORA – B3LYP / ANO-DK3 Unc.	2.0351	2.0375	2.1395	0.0210
	Experimental	**2.0250**	**2.0250**	**2.1800**	
$[Cu(C_6H_4S_2)_2]^{2-}$	x2c – B3LYP / x2c-QZVPPall	2.0123	2.0135	2.0443	0.0176
	x2c – B3LYP / ANO-DK3 Unc.	2.0133	2.0134	2.0358	0.0202
	ZORA – B3LYP / ANO-DK3 Unc.	2.0183	2.0198	2.0581	0.0095
	Experimental	**2.0190**	**2.0190**	**2.0850**	
$[Cu(C_6H_4Se_2)_2]^{2-}$	x2c – B3LYP / x2c-QZVPPall	2.0229	2.0452	2.0885	0.0129
	x2c – B3LYP / ANO-DK3 Unc.	2.0218	2.0475	2.0850	0.0121
	ZORA – B3LYP / ANO-DK3 Unc.	2.0322	2.0509	2.0906	0.0186
	Experimental	**2.0180**	**2.0180**	**2.0820**	

Table S14. Computed and experimental HFC constants of compounds **6–12**. Experimental values reported in the literature were given as absolute magnitudes.

Compound	Method	$A_{\perp}$ (MHz)	$A_{\perp}$ (MHz)	$A_{\parallel}$ (MHz)	MAPLE (%)
[Cu(Pc)]	x2c – B3LYP / x2c-QZVPPall	-47.6	-48.1	-634.8	28.6
	x2c – B3LYP / ANO-DK3 Unc.	-49.5	-50.0	-633.4	29.5
	ZORA – B3LYP / ANO-DK3 Unc.	-40.5	-41.0	-666.6	24.9
	Experimental	**15.0**	**15.0**	**630.0**	
$[V(C_6Br_4O_2)_3]^{2-}$	x2c – B3LYP / x2c-QZVPPall	-188.7	-331.1	40.9	6.0
	x2c – B3LYP / ANO-DK3 Unc.	-195.7	-340.2	21.2	11.0
	ZORA – B3LYP / ANO-DK3 Unc.	-195.4	-335.8	18.0	12.4
	Experimental	**280.0**	**365.0**	**60.0**	
$[V(C_6H_4O_2)_3]^{2-}$	x2c – B3LYP / x2c-QZVPPall	-246.1	-304.8	49.7	3.9
	x2c – B3LYP / ANO-DK3 Unc.	-255.5	-316.0	31.4	7.3
	ZORA – B3LYP / ANO-DK3 Unc.	-253.4	-310.9	28.7	8.1
	Experimental	**310.0**	**367.0**	**60.0**	
[Cu(acacen)]	x2c – B3LYP / x2c-QZVPPall	-59.9	-64.4	-634.2	0.7
	x2c – B3LYP / ANO-DK3 Unc.	-62.1	-66.6	-630.1	0.7
	ZORA – B3LYP / ANO-DK3 Unc.	-54.1	-57.1	-662.5	2.1
	Experimental	**63.0**	**63.0**	**650.0**	
[Cu(tmtaa)]	x2c – B3LYP / x2c-QZVPPall	-46.4	-43.2	-606.2	5.9
	x2c – B3LYP / ANO-DK3 Unc.	-49.5	-45.5	-605.9	4.9
	ZORA – B3LYP / ANO-DK3 Unc.	-38.8	-41.0	-635.0	7.5
	Experimental	**65.0**	**65.0**	**620.0**	
$[Cu(C_6H_4S_2)_2]^{2-}$	x2c – B3LYP / x2c-QZVPPall	-91.3	-95.9	-504.7	2.9
	x2c – B3LYP / ANO-DK3 Unc.	-45.5	-42.3	-421.6	14.5
	ZORA – B3LYP / ANO-DK3 Unc.	-72.3	-77.0	-525.0	6.4
	Experimental	**115.0**	**115.0**	**500.0**	
$[Cu(C_6H_4Se_2)_2]^{2-}$	x2c – B3LYP / x2c-QZVPPall	-136.9	-114.0	-453.0	2.1
	x2c – B3LYP / ANO-DK3 Unc.	-147.4	-121.5	-452.2	1.4
	ZORA – B3LYP / ANO-DK3 Unc.	-123.0	-143.6	-461.1	1.2
	Experimental	**145.0**	**145.0**	**460.0**	

S4. EPR Simulations

In our computational analysis, the magnitudes of the hyperfine coupling constants were found to be sufficient for interpreting the observed splitting. The signs of the HFC constants, however, were not determinative. Reversing the signs of the experimental coupling constants resulted in equivalent spectra, with no observable change as seen in Figure S1.

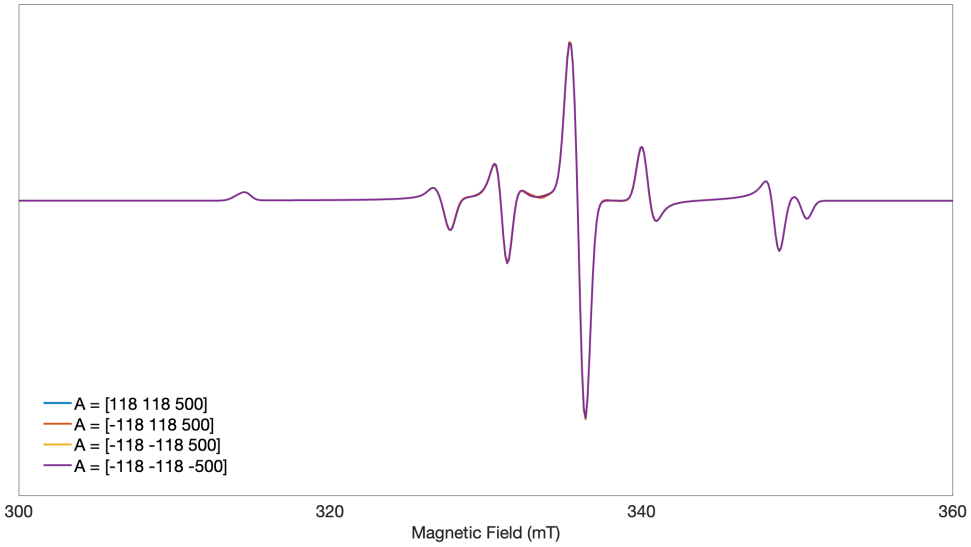

Figure S1. $[Cu(mnt)_2]^{2-}$ computed cw-EPR spectra using experimental EPR parameter values showing no differences upon sign reversal of one and multiple HFC components.

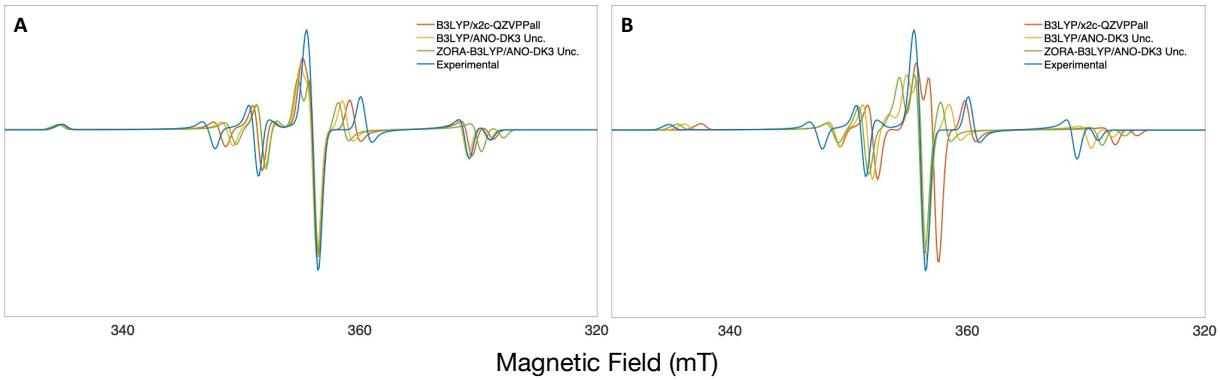

Figure S2. Simulated cw-EPR spectra of $[Cu(mnt)_2]^{2-}$ using EasySpin version 6.0. **A.** Comparison between computed and experimental hyperfine coupling constants setting experimental g-values. **B.** Comparison between computed and experimental EPR parameters.

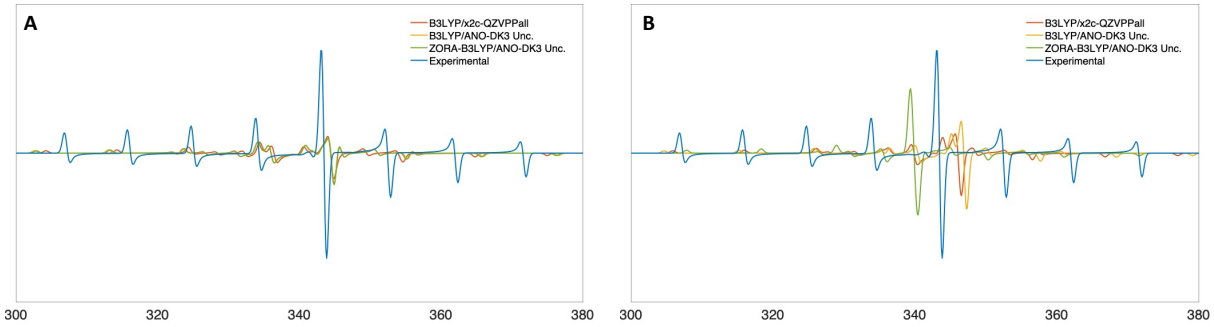

Figure S3. Simulated cw-EPR spectra of $[V(C_8S_8)_3]^{2-}$ using EasySpin version 6.0. **A.** Comparison between computed and experimental hyperfine coupling constants setting experimental g-values. **B.** Comparison between computed and experimental EPR parameters.

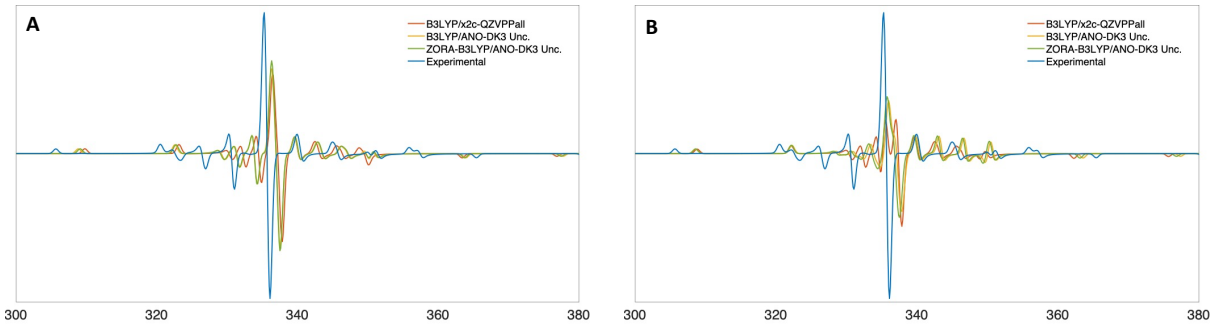

Figure S4. Simulated cw-EPR spectra of $[VO(dmit)_2]^{2-}$ using EasySpin version 6.0. **A.** Comparison between computed and experimental hyperfine coupling constants setting experimental g-values. **B.** Comparison between computed and experimental EPR parameters.

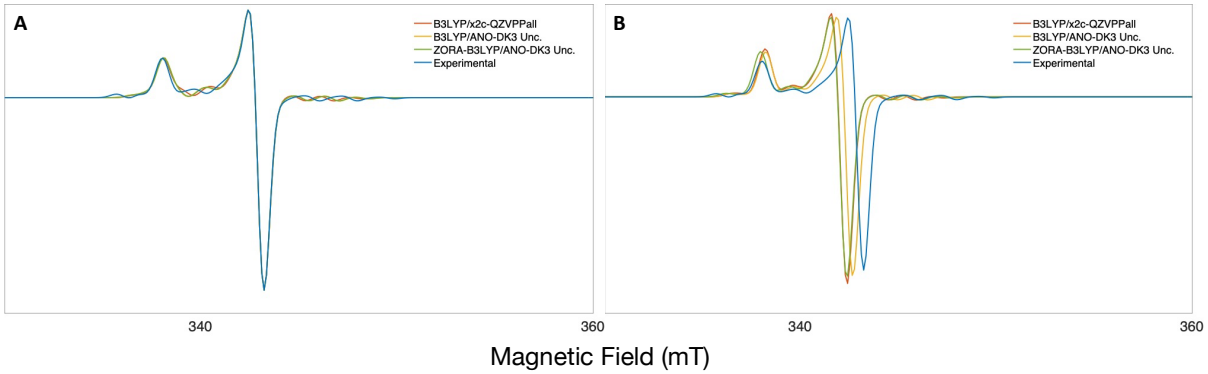

Figure S5. Simulated cw-EPR spectra of [CpTi(cot)] using EasySpin version 6.0. **A.** Comparison between computed and experimental hyperfine coupling constants setting experimental g-values. **B.** Comparison between computed and experimental EPR parameters.

S5. Hyperfine Coupling Decomposition

Table S15. Molecular orbital (MO) nucleus spin density contributions for compounds **1–5**. All calculations have been performed using an uncontracted version of ANO–DK3, B3LYP functional and ZORA relativistic treatment.

Compound	MO	[a]Spin up (α)	[a]Spin down (β)	Net Contribution
$[Cu(mnt)_2]^{2-}$	0 (1s)	10448.709928	-10448.724063	-0.014135
	5 (2s)	987.518789	-987.979931	-0.461142
	37 (3s)	144.188654	-143.846839	0.341815
	67 (valence)	0.161240	0.175200	-0.01396
	70 (valence)	0.605247	0.00000	0.605247
	71 (valence)	0.000000	-0.729916	-0.729916
	75 (valence)	0.000000	-0.075463	-0.075463
	78 (valence)	1.615801	-1.603239	0.012562
$[V(dmit)_3]^{2-}$	0 (1s)	4502.639159	-4502.644249	-0.005090
	16 (2s)	396.445869	-369.903024	-0.457155
	89 (3s)	54.925780	-54.769801	0.155979
	108 (valence)	0.195342	0.177957	0.017385
	117 (valence)	0.403931	0.355959	0.047972
	123 (valence)	0.251606	0.238234	0.013372
	138 (valence)	0.034361	0.010272	0.024089
	141 (valence)	0.939877	0.967312	-0.027435
	146 (valence)	0.021944	0.000005	0.021939
	148 (valence)	0.046414	0.000076	0.046338
$[V(C_8S_8)_3]^{2-}$	0 (1s)	4502.627895	-4502.632244	-0.004349
	25 (2s)	396.468339	-396.869749	-0.401410
	149 (3s)	54.954160	-54.812086	0.142074
	183 (valence)	0.187306	-0.175321	0.011985
	191 (valence)	0.027886	-0.017480	0.010406
	206 (valence)	0.065093	-0.006613	0.05848
	207 (valence)	0.011189	-0.046762	-0.035573
	209 (valence)	0.025606	-0.015535	0.010071
	219 (valence)	0.122479	-0.088172	0.034307
	222 (valence)	0.136319	-0.100649	0.03567
	223 (valence)	0.045072	-0.108819	-0.063747
	247 (valence)	0.109832	-0.003168	0.106664
	249 (valence)	0.135940	-0.024933	0.111007
	250 (valence)	0.000975	-0.015337	-0.014362
	251 (valence)	0.587423	-0.533436	0.053987
	252 (valence)	0.007914	-0.330686	-0.322772
	255 (valence)	0.016752	-0.004180	0.012572

	256 (valence)	0.043594	-0.005455	0.038139
	257 (valence)	0.040540	-0.000732	0.039808
	270 (valence)	0.012393	-0.001820	0.010573
$[VO(dmit)_2]^{2-}$	0 (1s)	4502.612219	-4502.615754	-0.003535
	11 (2s)	396.479722	-396.839240	-0.359518
	62 (3s)	54.757190	-54.623186	0.134004
	83 (valence)	0.149841	-0.128581	0.021260
	87 (valence)	0.177812	-0.162952	0.014860
	98 (valence)	0.386372	-0.534790	-0.148418
	102 (valence)	1.028937	-0.883105	0.145832
	112 (valence)	0.029750	-0.046213	-0.016463
	113 (valence)	0.057775	0.000000	0.057775
CpTi(cot)	0 (1s)	3873.540986	-3873.543185	-0.002199
	1 (2s)	335.768406	-336.027912	-0.259506
	18 (3s)	45.187734	-45.135144	0.05259
	42 (valence)	0.787415	0.742477	0.044938
	48 (valence)	0.027784	0.00000	0.027784
	49 (valence)	0.000000	0.022982	-0.022982
	56 (valence)	0.028570	0.000000	0.02857

[a]Electron density within the nucleus given in $a.u.^{-3}$

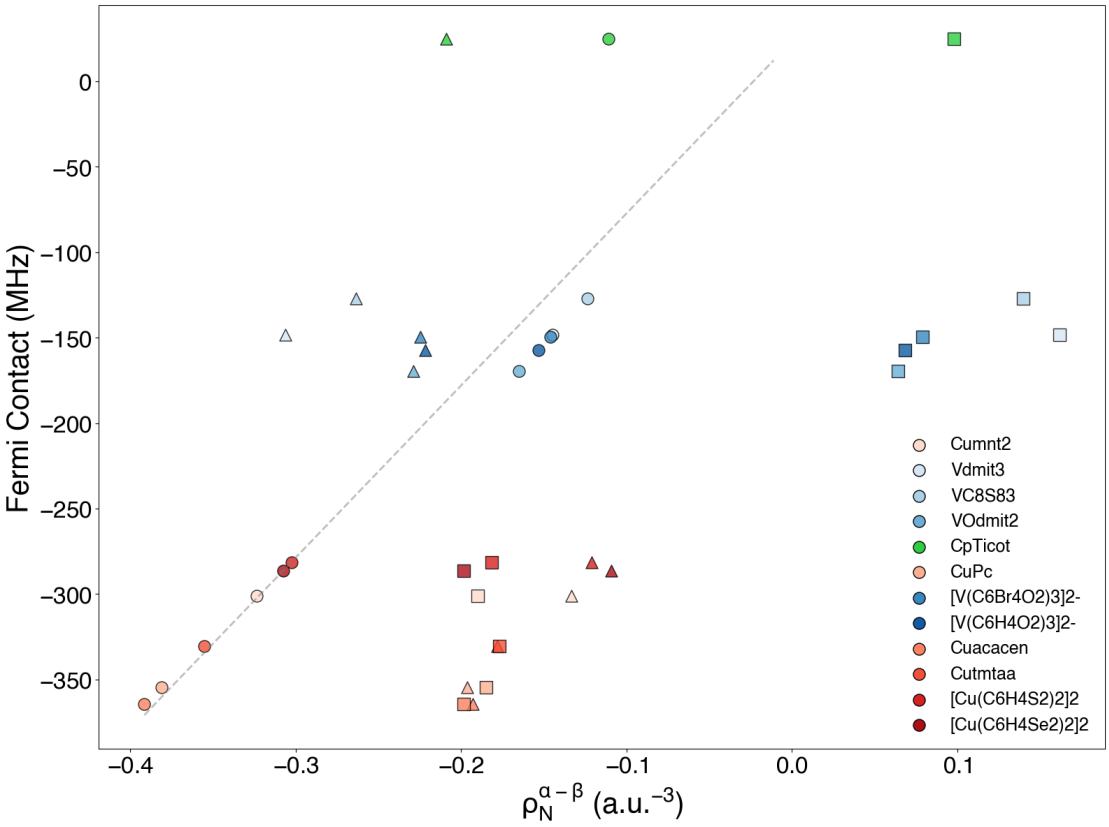

Figure S6. Correlation between isotropic term and nuclear spin density for compounds **1–12** Squares represent valence shell contributions, triangles represent core shell contributions and circles show the total contribution. Calculations were carried out employing B3LYP/ANO – DK3 and using ZORA relativistic treatment.

Table S16. Main axis values of the one-center reduced field gradient integral for all d orbitals in d^1 and d^9 systems (derived from Equation 6).

Orbital	f_{xx}	f_{yy}	f_{zz}
d_{z^2}	$-\frac{2}{7}$	$-\frac{2}{7}$	$\frac{4}{7}$
$d_{x^2-y^2}$	$\frac{2}{7}$	$\frac{2}{7}$	$-\frac{4}{7}$
d_{xy}	$\frac{2}{7}$	$\frac{2}{7}$	$-\frac{4}{7}$
d_{xz}	$\frac{2}{7}$	$-\frac{4}{7}$	$\frac{2}{7}$
d_{yz}	$-\frac{4}{7}$	$\frac{2}{7}$	$\frac{2}{7}$

Table S17. Nucleus spin density contribution per MO for model compounds. All calculations have been performed using an uncontracted version of ANO–DK3, B3LYP functional and ZORA relativistic treatment.

Geometry	V–N (Å)	MO	[a]Spin up (α)	[a]Spin down (β)	Net Contribution
Trigonal Plana (C_{3v})	2.046	0 (1s)	4502.881567	-4502.884883	-0.003316
		1 (2s)	396.486006	-396.958045	-0.472039
		8 (3s)	55.426090	-55.248623	0.177467
		21 (Valence)	1.038184	-1.309788	-0.271604
		23 (Valence)	0.364384	-0.141717	0.222667
Vacant Tetrahedra (C_{3v})	2.039	0 (1s)	4502.889341	-4502.891425	-0.002084
		1 (2s)	396.494591	-396.954028	-0.459437
		8 (3s)	55.349062	-55.165414	0.183648
		21 (Valence)	0.000000	-0.914056	-0.914056
		22 (Valence)	0.269175	0.000000	0.269175
		23 (Valence)	1.406725	-0.705276	0.701449
Square Planar (D_{4h})	2.044	0 (1s)	4502.814581	-4502.822431	-0.007850
		1 (2s)	396.443544	-396.848978	-0.405434
		9 (3s)	55.532431	-55.335805	0.196626
		25 (Valence)	1.288550	-1.382685	-0.094135
Tetrahedra (T_d)	2.041	0 (1s)	4502.851152	-4502.852626	-0.001474
		1 (2s)	396.495877	-396.906534	-0.410657
		9 (3s)	55.347576	-55.176533	0.171043
		25 (Valence)	0.000001	-2.084104	-2.084103
		26 (Valence)	2.234185	0.000000	2.234185
Seesaw (C_{2v})	2.043	0 (1s)	4502.828544	-4502.832793	-0.004249
		1 (2s)	396.478098	-396.876716	-0.398618

		9 (3s)	55.451836	-55.288075	0.163761
		25 (Valence)	0.368582	-1.240754	-0.872172
		26 (Valence)	1.598900	0.000000	1.598900
		27 (Valence)	0.000004	-0.659504	-0.659500
Trigonal Bipyramid (D_{3h})	2.130	0 (1s)	4502.836985	-4502.839489	-0.002504
		1 (2s)	396.474058	-396.891429	-0.417371
		10 (3s)	55.394308	-55.219679	0.174629
		29 (Valence)	1.909240	-1.818869	0.090371
		30 (Valence)	0.214384	-0.000562	0.213822
		31 (Valence)	0.000019	-0.150680	-0.150661
Square–Based Pyramid (C_{4v})	2.130	0 (1s)	4502.850230	-4502.852036	-0.001806
		1 (2s)	396.486758	-396.912551	-0.425793
		10 (3s)	55.383352	-55.212341	0.171011
		29 (Valence)	1.901437	-1.817364	0.084073
		30 (Valence)	0.109532	-0.047630	0.061902
Octahedra (O_h)	2.168	0 (1s)	4502.794879	-4502.799909	-0.005030
		1 (2s)	396.453790	-396.842953	-0.389163
		11 (3s)	55.544124	-55.371362	0.172762
		33 (Valence)	2.039398	-1.959323	0.080075
		34 (Valence)	0.037364	-0.009877	0.027487
Trigonal Prism (D_{3h})	2.169	0 (1s)	4502.836799	-4502.839426	-0.002627
		1 (2s)	396.483245	-396.895257	-0.412012
		11 (3s)	55.422486	-55.253644	0.168842
		33 (Valence)	1.859865	-1.749548	0.110317
		39 (Valence)	0.059215	0.000000	0.059215
Pentagonal Bipyramid (D_{5h})	2.220	0 (1s)	4502.828735	-4502.833860	-0.005125
		1 (2s)	396.472667	-396.881226	-0.408559
		12 (3s)	55.419224	-55.250134	0.169090
		37 (Valence)	1.699837	-1.604260	0.095577
		38 (Valence)	0.126792	-0.104168	0.022624
Capped Octahedra (C_{3v})	2.230	0 (1s)	4502.835896	-4502.841555	-0.005659
		1 (2s)	396.482765	396.887559	-0.404794
		12 (3s)	55.419447	55.247795	0.171652
		37 (Valence)	1.779315	-1.667743	0.111572

[a]Electron density within the nucleus given in $a.u.^{-3}$

Table S18. Spin Dipolar Component, SOMO and orbital spatial symmetry for Vanadium model compounds. All calculations have been performed using an uncontracted version of ANO–DK3, B3LYP functional and ZORA relativistic treatment.

Compound	A_{xx}	A_{yy}	A_{zz}	SOMO
Trigonal Planar	106.2	-199.7	93.5	d_{xz}
Vacant Tetrahedra	109.6	96.2	-205.9	d_{xy}
Square Planar	111.4	111.4	-222.8	d_{xy}
Tetrahedra	-104.3	-104.3	208.6	d_{z^2}
Trigonal Bipyramid	105.5	-210.5	104.9	d_{xz}
Square-Based Pyramid	103.8	103.8	-207.6	d_{xy}
Octahedra	108.5	107.3	-215.8	d_{xy}
Trigonal Prism	-111.4	-112.7	225.1	d_{z^2}
Pentagonal Bipyramid	-201.4	115.5	85.9	d_{yz}
Capped Octahedra	107.1	101.1	-208.2	$d_{x^2-y^2}$

Structures were generated using Shapes 2.1 substituting V–N bond lengths for optimized ones from same-numbered ligand optimized compounds.

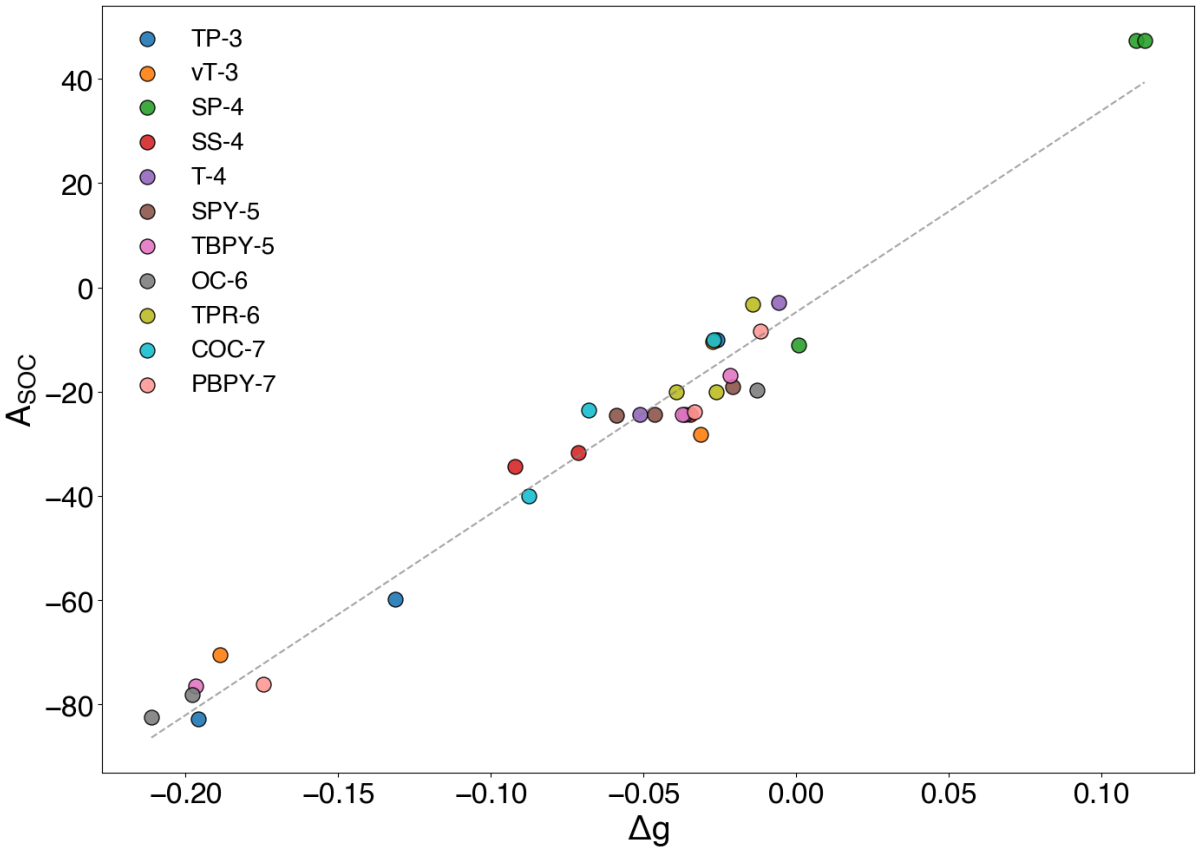

Figure S7. $\Delta g_{\mu\nu}$ against $\mathbf{A}_{\mu\nu}^{soc}$ (where $\mu = \nu$) for model compounds.